



Published in final edited form as:

Oncogene. 2018 April ; 37(14): 1926–1938. doi:10.1038/s41388-017-0091-1.

The miR-17/92 cluster is involved in the molecular etiology of the SCLL syndrome driven by the BCR-FGFR1 chimeric kinase

Tianxiang Hu, Yating Chong, Haiyan Qin, Eiko Kitamura, Chang-Sheng Chang, Jeane Silva, Mingqiang Ren¹, and John K Cowell

Georgia Cancer Center, Augusta University, Augusta, GA 30912

Abstract

MicroRNAs have pathogenic roles in the development of a variety of leukemias. Here we identify miRNAs that have important roles in the development of B-lymphomas resulting from the expression of the chimeric BCR-FGFR1 kinase. The miR-17/92 cluster was particularly implicated and forced expression resulted in increased cell proliferation, while inhibiting its function using microRNA sponges reduced cell growth and induced apoptosis. Cells treated with the potent BGJ389 FGFR1 inhibitor led to miR-17/92 downregulation suggesting regulation by FGFR1. Transient luciferase reporter assays and qRT-PCR detection of endogenous miR-17/92 expression in stable transduced cell lines demonstrated that BCR-FGFR1 can regulate miR-17/92 expression. This positive association of miR-17/92 with BCR-FGFR1 was also confirmed in primary mouse SCLL tissues and primary human CLL samples. miR-17/92 promotes cell proliferation and survival by targeting CDKN1A and PTEN in B-lymphoma cell lines and primary tumors. An inverse correlation in expression levels was seen between miR-17/92 and both CDKN1A and PTEN in two cohorts of CLL patients. Finally, *in vivo* engraftment studies demonstrated that manipulation of miR-17/92 was sufficient to affect BCR-FGFR1 driven leukemogenesis. Overall, our results define miR-17/92 as a downstream effector of FGFR1 in BCR-FGFR1 driven B cell lymphoblastic leukemia.

Keywords

microRNA; leukemia; AML; progression; FGFR1; BCR

INTRODUCTION

Lymphoid and myeloid malignancies associated with FGFR1 abnormalities, commonly referred to as stem cell leukemia/lymphoma syndrome (SCLL), is a rare but aggressive hematological neoplasm caused by chromosome rearrangements fusing the fibroblast growth

Users may view, print, copy, and download text and data-mine the content in such documents, for the purposes of academic research, subject always to the full Conditions of use: http://www.nature.com/authors/editorial_policies/license.html#terms

Corresponding author: John K. Cowell, Georgia Cancer Center, CN2119, 1120 15th Street, Augusta GA 30912. jcowell@augusta.edu, Tel: 706-721-5653, Fax: 706-721-0469.

¹Present address: Consortium for Health and Military Performance (CHAMP), Department of Military and Emergency Medicine, Uniformed Services University of the Health Sciences, 4301 Jones Bridge Road, Bethesda, MD 20814

Conflict of Interest statement: The authors declare no conflicts of interest associated with this work.

factor receptor 1 (FGFR1) gene on chromosome 8p11, with a variety of different partner genes.^{1,2} The resultant chimeric genes encode a constitutively activated FGFR1 tyrosine kinase, leading to activation of multiple downstream signal transduction pathways. This syndrome usually presents as a chronic myeloproliferative disorder at the time of diagnosis, but can rapidly progress to acute myeloid leukemia (AML), and is frequently associated with the coincident development of T- or B-cell lymphomas.^{3,4} A better understanding of molecular events involved in SCLL, therefore, is required to understand the molecular etiology of the disease and develop more effective treatments.

A series of SCLL mouse models have been developed through transduction of normal bone marrow cells with different, chimeric FGFR1 kinases followed by their transplantation into healthy donors, which recapitulate the phenotypic and genotypic features of SCLL.^{3,5-8} Transformed human CD34+ cells engrafted into immunocompromised mice also develop SCLL.⁹⁻¹¹ Perhaps the most aggressive variant of SCLL is associated with the BCR-FGFR1 chimeric kinase, resulting from a t (8; 22) chromosome translocation,¹² which is distinguished by associated B-cell lymphomas. Syngeneic mouse models of BCR-FGFR1 SCLL develop pre-B-cell lymphomas⁸ and human CD34+ cells transformed with BCR-FGFR1 develop AML in immunocompromised mice.⁹

MicroRNAs are short, non-coding RNAs (19–23 nt) that either impair translation, or induce degradation of mRNA targets through complementary pairing, typically within the 3' untranslated region.¹³ MicroRNAs have been associated with the development of several types of AML¹⁴⁻¹⁶ but no studies report micro-RNA profiles in the development of SCLL disease. Here we define FGFR1 driven miRNA profile changes related to SCLL development and in particular show that the miR-17/92 cluster is regulated by BCR-FGFR1, leading to increased cell proliferation and suppression of apoptosis. We also demonstrate that miR-17/92 acts, at least partially, through targeting CDKN1A and PTEN.

RESULTS

Identification of miR-17/92 as a downstream target of BCR-FGFR1

The BBC1 and BBC2 cell lines were isolated from pre-B-cell lymphoma models of a murine BCR-FGFR1 driven SCLL.⁸ miRNA profiles for these cells, were established using miRNA arrays. First, BBC2 cells were compared with FACS sorted, normal, murine splenic CD19+ B cells isolated from BALB/c mice, where 191 miRNAs were upregulated and 59 were downregulated in BBC2 cells (Figure 1A and supplemental tables 1 and 2). We next investigated which of these miRNAs were affected by loss of FGFR1 function. Previously we showed that the FGFR inhibitor BGJ398 suppressed phosphoactivation of chimeric FGFR1 kinases.¹⁹ When BBC2 cells were treated with 15nM BGJ398 for 48 hours, 59 miRNAs were downregulated and 43 were up-regulated (Figure 1A and supplemental tables 1 and 2). Of the miRNAs dysregulated in the BBC2/CD19+ comparison, 33 miRNAs activated in BBC2 were downregulated by BGJ398, and 13 suppressed miRNAs were upregulated (Figure 1A). This analysis defined 46 core miRNAs which appear to be regulated by BCR-FGFR1 (Figure 1B).

Further analysis of these 46 miRNAs (Figure 1B) showed that 8/33 of the core up-regulated group (miR-18a-5p, miR-18b-5p, miR-19a-3p, miR-19b-3p, miR-20a-5p, miR-20b-3p, miR-20b-5p and miR-92b-3p) belonged to a 16-member family, comprising miR-92b and three paralogous clusters, miR-17~92, miR-106a-363 and miR-106b-25.²⁰ The overrepresentation of miR-17~92 family miRNAs within the core group suggests their possible roles in the etiology of SCLL. In addition, a pilot analysis of 12 candidate miRNAs, selected based on their potential association with cancer,²¹ revealed that 8/12 promoted cell growth, with the highest effect observed for the 3 miRNAs from the miR-17/92 cluster (Supplemental Figure 1). We, therefore, focused our functional studies on miR-17/92 cluster in BCR-FGFR1 driven lymphoblastic leukemia.

Expression levels of the miR-17/92, miR-106a/363 and miR-106b/25 clusters in BBC2 cells, relative to normal CD19+ cells, are shown in Figures 1C–E. The miR-17/92 and miR-106a/363 clusters seem more closely associated with disease progression, compared with the miR-106b/25 cluster, which is not activated in BBC2 cells. Consistently, BGJ398 treatment significantly reduced miR-19b and miR-20a/b expression (Figure 1F). In addition, miR-92a, which was not identified in the cross comparison with CD19+ cells, also showed a highly significant reduction in BBC2 after BGJ398 treatment, even though the fold change was relative small. In contrast, miR-25a, located in the miR-106b/25 cluster, did not show any change in expression levels after BGJ398 treatment (Figure 1F).

Forced expression of miR-17/92 promotes cell proliferation

To investigate the effects of miR-17/92 cluster on proliferation, the ~200bp core sequence containing the pri-miRNA and minimal ~100bp flanking sequence was cloned into the GFP-expressing pMSCV-PIG retrovirus vector²² and introduced into BBC2 cells, to develop cell lines stably coexpressing GFP. For each member of the miRNA cluster (miR-19b-3p, miR-20a-5p and miR-92a-3p), overexpression was validated by RT-PCR, where expression level increases ranged from 40–196 fold (Figure 2A). In cell growth competition assays (Supplemental Figure 1A),²³ BBC2 cells expressing the exogenous miRNA (GFP+), co-seeded 1:1 with parental (GFP–) cells, showed increased GFP+/GFP– ratios for miR-19b (91.19%), miR-20a (92.68%) or miR-92a (81.76%) respectively (Figure 2G) over a 12-day period compared with control cells (~50%).

Trypan blue dye exclusion analysis of BBC2 cells transduced with miR-19b, miR-20a and miR-92a showed increased cell numbers after 3 days in all cases, compared with empty vector transduced cells (Figure 2B). Similarly, luminescent cell viability assays demonstrated that the same transduced BBC2 cells showed increased growth levels (Figure 2C). This effect on growth was confirmed in another independent BCR-FGFR1 driven B-cell lymphoblastic leukemia cell line, BBC1,⁸ with significant increases in cell proliferation as measured by both trypan blue exclusion and cell viability assays (Figure 2 D–F).

To investigate how the forced expression of the miR-17/92 cluster promotes growth, we examined cell cycle progression in BBC2 cells overexpressing miR-19b, miR-20a and miR-92a using Hoechst 33342 staining.²⁴ As shown in Figure 2H, forced expression of miR-19b, miR-20a and miR-92a in BBC2 cells, increased the proportion of cells in G2/M

(Figure 2I), and decreased cells in the G0/G1 phase. There were no statistically significant differences in the proportion of cells in S-phase.

Inhibition of miR-17/92 reduced cell proliferation and induced apoptosis

MicroRNA sponges contain multiple tandem binding sites to a microRNA of interest which inhibits their function.²⁵ When miR-19b-3p (miR-19bSP), miR-20a-5p (miR-20aSP) and miR-92a-3p (miR-92aSP) were inhibited either individually, or in a combination sponge against all three (combiSP), GFP competition assays showed that the transduced BBC2 cells were out-grown by the GFP- cells after 12 days in all cases (Figure 3A). Reduced cell proliferation and viability were observed in the BBC2 cells transduced with miR-19bSP, miR-20aSP, miR-92aSP and combiSP (Figures 3A–C). Cell cycle analysis showed that miR-19bSP, miR-20aSP, miR-92aSP and CombiSP, decreased the ratio of cells in the S/G2/M phases (Figure 3D, F). In addition, 7 days after transduction, BBC2 cells transduced with miRNA sponge constructs showed 2.63–5.77-fold increases in Annexin V+/7-AAD– cells compared to empty vector transduced cells (Figure 3E, G), and 1.61–3.05-fold increases in total Annexin V+ cells (Supplemental Figure 2A, B), which demonstrated that miR-17/92 functions not only to promote cell proliferation, but also to maintain cell survival by suppressing apoptosis.

Overexpression of miR-17/92 rescues the effects of BGJ398 inhibition

If miR-17/92 functions downstream of BCR-FGFR1 to promote tumor cell transformation, then its overexpression should make cells more resistant to FGFR1 inhibition. When FGFR1 signaling was blocked using 15nM BGJ398 for 48 hours in control cells, as well as cells overexpressing miR-19b, miR-20a and miR-92a, cell cycle progression was significantly inhibited, with a reduction in the proportion of cells in S/G2/M, compared with the DMSO treated control (Figure 4A, B). As expected, overexpression of miR-19b, miR-20a and miR-92a rescued these cells from cell cycle arrest. Moreover, overexpression of miR-19b, miR-20a and miR-92a also reduced sensitivity to BGJ398-induced apoptosis (Figure 4C). In BBC2 cells transduced with the empty vector control, and treatment with BGJ398 increased the proportion of cells expressing the early Annexin V+/7-AAD- apoptotic markers by an average of 2.74-fold, from 2.95% to 8.09% ($p=1.70e-03$) (Supplemental Figure 2C), and Annexin V+/7-AAD+ late apoptotic markers by 6-fold, from 3.5% to 20.97% ($p=2.16e-05$) (Figure 4D). Overexpression of miR-19b, miR-20a and miR-92a significantly reduced the proportion of cells in late stages of apoptosis (Figure 4D) with less significant change for cells in early apoptosis (Supplemental Figure 2C, D).

To further investigate the protective effect of the miR-17/92 cluster against FGFR1 signal inhibition, we performed GFP competition assays after treatment with different concentrations of BGJ398. As shown in Figure 4E and F, overexpression of miR-20a and miR-92a provided a survival advantage after treatment with FGFR inhibitors using the GFP competition assay where, after 9 days, the GFP+ population in miR-20a overexpressing BBC2 cells increased significantly in dose-dependent manner (Figure 4E). Similarly, overexpression of miR-92a led to a significant, dose-dependent increase (78–88%) (Figure 4F). Consistently, inhibition of the miR-17/92 cluster significantly sensitized the cells to FGFR1 inhibition (Figure 4G). Importantly, this effects were related to the expression levels

of miR-17/92, as mirrored by the co-expressed GFP. The enrichment of GFP+ miR-92a expressing cells during the course was accompanied with the increase of mean fluorescence intensity (MFI), while depletion of GFP+ miR-17/92 sponged cells showed a reduced MFI, suggesting the protective effect was directly correlated to the miR-17/92 expression (supplemental Figure 2E).

BCR-FGFR1 regulates miR-17/92 expression in vitro and in vivo

To investigate whether miR-17/92 is regulated by BCR-FGFR1, we performed luciferase-based reporter assays. The miR-17/92 promoter was cloned into pGL3 and transfected into 293FT cells. Compared with the empty pGL3 or pMSCV vectors, which showed only baseline expression of luciferase, co-transfection of the microRNA promoter with BCR-FGFR1 led to increased luciferase expression proportional to BCR-FGFR1 levels, confirming this microRNA cluster is activated by the fusion kinase (Figure 5A). In addition, NIH3T3 and BaF3 cells stably expressing BCR-FGFR1 showed significant upregulation of endogenous miR-19b-3p, miR-20a-5p (Figure 5B). The activation of miR-17/92 associated with expression of the BCR-FGFR1 fusion kinase was further confirmed in bone marrow cells from murine BCR-FGFR1 induced B-lymphoblastic leukemias,⁸ compared with bone marrow cells from normal mice (Figure 5C).

To investigate the relationship between FGFR1 expression and miR-17/92 in primary human samples, we analysed data from two independent B-CLL patient cohorts (GSE40571 and GSE51529).^{26,27} Firstly, we ranked the samples according to FGFR1 expression levels, and selected the first quartile with highest expression and the fourth quartile with the lowest expression levels (Supplemental Figure 3A–D). When the expression of target miRNAs was compared in the FGFR1 high and low groups from both cohorts (Figure 5D), miR-19b-3p and miR-20a-5p consistently showed significantly higher expression in the FGFR1 high group. miR-92a-3p showed a less significantly higher expression level ($p=2.61e-02$) in GSE40571, and significantly higher expression ($p=1.47e-03$) in GSE51529. In contrast, in the same analysis comparing miR-19b-3p, miR-20a-5p and miR-92a-3p with actin high and low expressers, there was no significant difference (Supplemental Figure 3E).

CDKN1A and PTEN are direct targets of miR-17/92 in B cell leukemogenesis

Analysis of expression changes of several known miR-17/92 targets, such as BIM, CDKN1A, MYCC, E2F2 and PTEN²⁸ following either overexpression or inhibition of miR-17/92 (Figure 6A–D, F, G and Supplementary Figure 4A) showed that, in BBC2 cells ectopically overexpressing miR-20a, CDKN1A mRNA levels were down regulated 5.41 fold ($p=3.89e-06$). Consistently, CDKN1A expression was up regulated 3.64-fold ($p=5.04e-03$) in miR-20a-5p inhibited cells (Figure 6B). This direct targeting effect of CDKN1A by miR-20a-5p was also confirmed by western blotting (Figure 6F). Although expression of BIM, MYCC, E2F2 and PTEN was unaffected by miR-20a-5p, it was interesting to note that PTEN was targeted by both miR-19b-3p and miR-92a-3p (Supplemental Figure 4A). Compared with BIM and MYCC, PTEN was directly regulated by miR-19b and miR-92a, with significant suppression in overexpressing cells, and increased expression in sponge-inhibited cells (Figure 6 C, D and G).

Analysis of bone marrow cells from primary BCR-FGFR1 induced SCLL mouse models, showed expression of CDKN1A and PTEN were much lower than in the corresponding control tissue (Figure 6E and H). Importantly, there was a significant inverse correlation between miR-20a-5p and CDKN1a expression (Figure 6I) in the two B-CLL cohorts ($p=2.40e-02$ and $p=2.52e-02$, respectively). Moreover, an even more significant inverse correlation between miR-92a-3p and PTEN expression was detected in these primary CLL samples (both $p<1.00e-04$). There was, however, no correlation between the expression of miR-19b-3p and PTEN, possibly because of its relatively weaker effect (Figure 6C and D).

miR-17/92 promotes BCR-FGFR1 driven disease progression in vivo

To evaluate the possible oncogenic effect of miR-17/92 in BCR-FGFR1 driven leukemogenesis in vivo, 2×10^6 BBC2 cells, either stably overexpressing the miR-20a, miR-92a miRNAs or the combined sponge inhibitors, were injected into the tail veins of 6- to 8-week old ($n=5$), sub-lethally irradiated, syngeneic BALB/c mice (Figure 7A) as described previously.²⁹ Aggressive disease developed within 10–20 days and all mice showed high levels of GFP+ cells in the peripheral blood as early as one week after injection (Figure 7B). Consistent with the in vitro cell proliferation effects, overexpression of miR-20a and miR-92a increased the proportion of GFP+ BBC2 cells in peripheral blood from 50.93% to 76.78% ($p=3.94e-04$) and 83.58% ($p=2.03e-04$), respectively, while inhibition of miR-17/92 function decreased the GFP+ cell proportion to 28.95% ($p=2.36e-03$) one week after transplantation (Figure 7C). In addition, the mice transplanted with the BBC2 cells with forced expression of miR-20a and miR-92a, displayed significantly enlarged spleens and the mice injected with miR-17/92 sponged BBC2 cells showed reduced spleen size, compared with empty vector control (Figure 7D, and supplemental figure 5A). Consistently, the smaller spleens from mice engrafted with miR-17/92 inhibited BBC2 cells showed fewer GFP+ cells compared with the other constructs (Supplemental Figure 5B). Moreover, mouse survival data further confirmed the promotion of leukemogenesis by the miR-17/92 cluster, where survival time was significantly prolonged in the sponge transduced cell group, while significantly shortened in the miR-20a and miR-92a overexpressing group (Figure 7E). These data further demonstrated the importance of the miR-17/92 cluster in SCLL induced by the chimeric BCR-FGFR1 kinase.

DISCUSSION

Signaling by the mammalian Fibroblast Growth Factor (FGF) family, comprising eighteen secreted proteins that interact with four signaling tyrosine kinase FGF receptors (FGFRs), is important in multiple biological processes including pro-survival signals, anti-apoptotic signals and stimulation of cell proliferation and migration.³⁰ Moreover, genetic alterations in FGFs and FGFRs have been described in different cancer types, including breast cancer, ovarian cancer, bladder cancer, gastric cancer, myeloma and SCLL. While most studies have focused on four major downstream intracellular signaling pathways, RAS-MAPK, PI3K-AKT, PLC γ and signal transducer and activator of transcription (STAT), to our knowledge, this is the first unbiased global screen to identify FGFR1 regulated miRNA networks. Here, we present a summary of FGFR1-regulated miRNAs to guide prioritization for further

validation and functional characterization, not only in B cell lymphoblastic leukemia, but also in different cancer types with abnormal FGFR signaling.

The FGF pathways can be regulated by miRNAs, through directly targeting the ligands or receptors.³¹ For example, miR-338 directly regulates FGFR2 expression in osteoblasts, miR-424 and miR-503 directly suppress FGF2 and FGFR1 expression in pulmonary artery endothelial cells, and miR-710 is a direct regulator of FGF15 expression in myofibroblasts. Dysfunction of miRNA regulation of FGF signaling can also result in cancer progression. In non-small-cell lung cancer (NSCLC), for example, down regulation of miR-152 and miR-198 leads to increased levels of FGF2 and FGFR1 respectively, leading to decreased apoptosis and increased proliferation and invasion. In breast cancer, reduced expression of miR-503 results in increased FGF8 and consequent increased angiogenesis and proliferation. In the present study, we identified 59 microRNAs that were up-regulated and 43 that were suppressed by FGFR1 signaling, including well known oncomiRNAs miR-27a,³² miR-210,³³ miR-155,³⁴ miR-483³⁵ and the miR-17/92 cluster.³⁶⁻⁴¹ In addition, miR-26a/b,⁴² miR-150,^{43,44} miR-433⁴⁵ and miR-503,⁴⁶ likely function as tumor suppressors in SCLL neoplasms. Consistent with this speculation, over expression of miR-17/92 only partially rescued the cells from BGJ398 induced cell cycle inhibition and apoptosis, implying the involvement of other miRNAs in FGFR1 fusion kinase driven SCLL. These observations reveal an integrative picture of microRNAs and components of the FGFR signaling pathway to orchestrate development and differentiation.

The mechanism underlying FGFR1 fusion kinase-driven SCLL has been investigated in both animal and cell models, including activation of the FGFR1 downstream intracellular signaling cascades including PLC γ , STAT5 and SRC,⁴⁷ and specific upregulation of FLT3, GF11 and KIT stem cell markers, while suppressing differentiation associated genes IRF8, CSF1R, KLF4 and SPI1 in lymphomagenesis induced by FGFR1 fusion genes.⁹⁻¹¹ Activation of the miR-17/92 cluster likely also contributes to lymphomagenesis, since miR-20a targets CDKN1A to counter cell cycle inhibition, and miR-19b and miR-92a reduce the expression of PTEN, which can promote cell survival and proliferation and prevent apoptosis. Importantly, these data suggest that the *in vivo* oncomiRNA activity of miR-17/92 is mediated by the cooperative and simultaneous repression of multiple tumor suppressors potentially important in the transformation and progression of SCLL.

Previous work has demonstrated crucial roles for miR-17/92 during tumorigenesis, not only of solid tumors, but also acute lymphoid and myeloid leukemias, chronic myeloid leukemia and B-cell lymphomas.²⁸ As one of the best-studied microRNA clusters, many mRNA targets have been identified in different models, including AML1, BCL2L11 (BIM), CDKN1A, CTGF, EGR2, E2Fs, IKAROS, PTEN, STATs and SMADs.^{28,37,48-50} However, the mechanisms that drives miR-17/92 expression in disease remain poorly understood, with limited regulators such as c-MYC/N-MYC, TP53 and E2F family members reported.²⁸ Here we provide direct evidence that FGFR1 is a regulator of the miR-17/92 cluster. In our reporter assay, we showed that FGFR1 can activate miR-17/92 with transient co-expression of BCR-FGFR1. In NIH3T3 and BaF3 cells stably transduced by BCR-FGFR1, the endogenous expression of miR-17/92 was also increased. Moreover, real-time qPCR also confirmed the increased expression of miR-17/92 in primary tumor tissue from murine

BCR-FGFR1 SCLL. Meanwhile, this positive association was also observed in two cohorts of primary human CLL samples. Together, these data suggest that FGFR1 is an activator of miR-17/92, and miR-17/92 may be widely involved in FGFR1 regulated development and disease processes, which can be validated in future studies.

In both SCLL cell and mouse disease models, miR-17/92 was shown to target and suppress PTEN and CDKN1A in BCR-FGFR1 driven B cell lymphoblastic leukemia. It was reported that miR-17/92 can target BIM, CDKN1A, E2F2, c-MYC and PTEN, while in our primary screen, both by real-time qPCR and western blotting, only CDKN1A and PTEN showed significant expression changes, which suggests that BIM, E2F2 and c-MYC may also be co-regulated by other mechanisms. The strong anti-correlation between miR-20a and CDKN1A, and miR-92a with PTEN, seen in the two CLL cohorts raises the possibility that miR-17/92 may be a specific target for disease treatment. Indeed, manipulation of the miR-17/92 cluster in FGFR1 fusion kinase driven B cell lymphoblastic leukemia impacted disease progression in a murine model supporting its role in FGFR1 driven B cell lymphoblastic leukemia.

In conclusion, we provide evidence that the BCR-FGFR1 fusion kinase activates miR-17/92 clusters, which in turn simultaneously targets tumor suppressors CDKN1A and PTEN, providing further insight into the molecular etiology of chimeric FGFR1 induction of SCLL, and possibly in other solid tumors showing FGFR1 amplification and overexpression.

MATERIALS AND METHODS

Molecular analyses

Precursor microRNAs were cloned into pMSCV- PIG (Addgene Plasmid #21654). MicroRNA sponge constructs were kindly provided by Dr. Kluiver.¹⁷ Quantitative reverse transcription polymerase chain reaction and western blotting assays were carried out as described previously.¹⁸

Retrovirus production and transduction

293FT cells were transfected with 2.5 µg of retroviral expression vector and 2.5 µg pCL-Eco vector (Addgene plasmid #12371) in 6 well format using lipofectamine (Invitrogen, Carlsbad, CA). Virus was harvested after 2 days and target cells were transduced with RetroNectin reagent (Clontech, Mountain View, CA) according to the manufacturer's protocol. 2 days after transduction, transduced cells were selected with 1 µg/ml puromycin to generate stable cell lines.

Cell analyses in vitro

Cells were cultured in RPMI 1640 medium containing 10% FBS. For GFP competition assay cells were mixed 1:1 and cultured for 12 days during which the percentage of GFP+ cells was determined using FACSCanto II flow cytometry (BD Biosciences, San Jose, CA). Cell viability was measured using the CellTiter-Glo Luminescent Cell Viability Assay (Promega, Madison, WI). Trypan blue exclusion analysis was performed using a Cellometer Auto 2000 Cell Viability Counter (Nexcelom, Lawrence, MA). For FGFR inhibition assays,

puromycin selected, stable cells were treated with 15nM of BGJ398 (Selleckchem, Houston, TX) for 48 h, followed by cell cycle and apoptosis assay.

miRNA profiling and analysis

miRNA was prepared using the mirVana miRNA Isolation Kit (Thermo Fisher Scientific, Waltham, MA). 250 ng of total RNA was labeled with biotin using the FlashTag Biotin HSR RNA Labeling Kit (Affymetrix, Santa Clara, CA) which was hybridized to the GeneChip miRNA 1.0 or miRNA 4.0 arrays (Affymetrix) according to the manufacturers' protocol. The primary .CEL files were imported into Partek Genomics Suite 6.6 (Partek, St. Louis, MO) for normalization using RMA (Robust Multi-array Average). Differential expression for each comparison was calculated using ANOVA and a differential gene expression list was generated using and FDR of 0.05 and expression alterations of $>1.5_{\log_2}$ -fold increases or decreases. Data presented have been deposited in the NCBI Gene Expression Omnibus (GEO) Series accession number GSE104894 and GSE104895.

Cell cycle and apoptosis analysis

10^6 cells were labeled with Hoechst 33342 (Thermo Fisher Scientific, Waltham, MA) for 1 hour at 37°C and cell cycle profiles were determined using the BD LSR II flow cytometer (BD Bioscience, San Jose, CA). To measure apoptosis, 10^6 cells were stained with APC Annexin V and DNA binding dye 7-amino-actinomycin (7-AAD) (Biolegend, San Diego, CA,) according to the manufacturer's protocol and analyzed by BD FACSCanto II flow cytometry (BD Bioscience, San Jose, CA).

Luciferase reporter assay

HEK293T cells were cultured overnight at 10^5 cells/500 μ l in each well of a 24-well plate. 400 ng of reporter plasmid derived from pGL3 was transfected with or without pMSCV-BCR-FGFR1 containing plasmid using 2 μ l of Lipofectamine 2000 (Invitrogen, Carlsbad, CA) according to manufacturer's protocol. Cells were harvested 48 h after transfection and analyzed using the Dual-Luciferase Reporter Assay System (Promega, Madison, WI). Renilla luciferase was used to normalize for transfection efficiency, and the ratio of firefly/Renilla luciferase activities is designated as relative promoter activity.

Mouse engraftment

6–8 week old female Balb/c mice (The Jackson Laboratory, Bar Harbor, ME) were injected with 2×10^6 BBC2 cells through the tail vein. One week after injection, the GFP+ cell population in the peripheral blood was analyzed using flow cytometry. All mice were evaluated daily for signs of morbidity, weight loss, failure to thrive, and splenomegaly. Premorbid animals were sacrificed by CO₂ asphyxiation, and then hematopoietic tissues were removed for subsequent analysis. All animal experiments were carried out under protocols approved by the Institutional Animal Care and Use Committee of the Augusta University.

Supplementary Material

Refer to Web version on PubMed Central for supplementary material.

Acknowledgments

This work was supported by grant CA076167 from the National Institutes of Health

References

1. Kumar KR, Chen W, Koduru PR, Luu HS. Myeloid and lymphoid neoplasm with abnormalities of FGFR1 presenting with trilineage blasts and RUNX1 rearrangement: a case report and review of literature. *Am J Clin Pathol.* 2015; 143:738–748. [PubMed: 25873510]
2. Macdonald D, Reiter A, Cross NC. The 8p11 myeloproliferative syndrome: a distinct clinical entity caused by constitutive activation of FGFR1. *Acta Haematol.* 2002; 107:101–107. [PubMed: 11919391]
3. Roumiantsev S, Krause DS, Neumann CA, Dimitri CA, Asiedu F, Cross NC, et al. Distinct stem cell myeloproliferative/T lymphoma syndromes induced by ZNF198-FGFR1 and BCR-FGFR1 fusion genes from 8p11 translocations. *Cancer Cell.* 2004; 5:287–298. [PubMed: 15050920]
4. Jackson CC, Medeiros LJ, Miranda RN. 8p11 myeloproliferative syndrome: a review. *Hum Pathol.* 2010; 41:461–476. [PubMed: 20226962]
5. Guasch G, Delaval B, Arnoulet C, Xie MJ, Xerri L, Sainy D, et al. FOP-FGFR1 tyrosine kinase, the product of a t(6;8) translocation, induces a fatal myeloproliferative disease in mice. *Blood.* 2004; 103:309–312. [PubMed: 12969958]
6. Ren M, Li X, Cowell JK. Genetic fingerprinting of the development and progression of T-cell lymphoma in a murine model of atypical myeloproliferative disorder initiated by the ZNF198-fibroblast growth factor receptor-1 chimeric tyrosine kinase. *Blood.* 2009; 114:1576–1584. [PubMed: 19506298]
7. Agerstam H, Jaras M, Andersson A, Johnels P, Hansen N, Lassen C, et al. Modeling the human 8p11-myeloproliferative syndrome in immunodeficient mice. *Blood.* 2010; 116:2103–2111. [PubMed: 20554971]
8. Ren M, Tidwell JA, Sharma S, Cowell JK. Acute progression of BCR-FGFR1 induced murine B-lympho/myeloproliferative disorder suggests involvement of lineages at the pro-B cell stage. *PLoS One.* 2012; 7:e38265. [PubMed: 22701616]
9. Cowell JK, Qin H, Chang CS, Kitamura E, Ren M. A model of BCR-FGFR1 driven human AML in immunocompromised mice. *Br J Haematol.* 2016; 175:542–545. [PubMed: 27785808]
10. Qin H, Wu Q, Cowell JK, Ren M. FGFR1OP2-FGFR1 induced myeloid leukemia and T-cell lymphoma in a mouse model. *Haematologica.* 2016; 101:e91–94. [PubMed: 26589915]
11. Ren M, Qin H, Wu Q, Savage NM, George TI, Cowell JK. Development of ZMYM2-FGFR1 driven AML in human CD34+ cells in immunocompromised mice. *Int J Cancer.* 2016; 139:836–840. [PubMed: 27005999]
12. Demiroglu A, Steer EJ, Heath C, Taylor K, Bentley M, Allen SL, et al. The t(8;22) in chronic myeloid leukemia fuses BCR to FGFR1: transforming activity and specific inhibition of FGFR1 fusion proteins. *Blood.* 2001; 98:3778–3783. [PubMed: 11739186]
13. Bartel DP. MicroRNAs: genomics, biogenesis, mechanism, and function. *Cell.* 2004; 116:281–297. [PubMed: 14744438]
14. Volinia S, Galasso M, Costinean S, Tagliavini L, Gamberoni G, Drusco A, et al. Reprogramming of miRNA networks in cancer and leukemia. *Genome Res.* 2010; 20:589–599. [PubMed: 20439436]
15. Marcucci G, Mrozek K, Radmacher MD, Garzon R, Bloomfield CD. The prognostic and functional role of microRNAs in acute myeloid leukemia. *Blood.* 2011; 117:1121–1129. [PubMed: 21045193]
16. Mavrakis KJ, Van Der Meulen J, Wolfe AL, Liu X, Mets E, Taghon T, et al. A cooperative microRNA-tumor suppressor gene network in acute T-cell lymphoblastic leukemia (T-ALL). *Nat Genet.* 2011; 43:673–678. [PubMed: 21642990]
17. Kluiver J, Gibcus JH, Hettinga C, Adema A, Richter MK, Halsema N, et al. Rapid generation of microRNA sponges for microRNA inhibition. *PLoS One.* 2012; 7:e29275. [PubMed: 22238599]

18. Teng Y, Mei Y, Hawthorn L, Cowell JK. WASF3 regulates miR-200 inactivation by ZEB1 through suppression of KISS1 leading to increased invasiveness in breast cancer cells. *Oncogene*. 2014; 33:203–211. [PubMed: 23318438]
19. Wu Q, Bhole A, Qin H, Karp J, Malek S, Cowell JK, et al. SCLLTargeting FGFR1 to suppress leukemogenesis in syndromic and de novo AML in murine models. *Oncotarget*. 2016; 7:49733–49742. [PubMed: 27391347]
20. Ota A, Tagawa H, Karnan S, Tsuzuki S, Karpas A, Kira S, et al. Identification and characterization of a novel gene, C13orf25, as a target for 13q31-q32 amplification in malignant lymphoma. *Cancer Res*. 2004; 64:3087–3095. [PubMed: 15126345]
21. Xie B, Ding Q, Han H, Wu D. miRCancer: a microRNA-cancer association database constructed by text mining on literature. *Bioinformatics*. 2013; 29:638–644. [PubMed: 23325619]
22. Mayr C, Bartel DP. Widespread shortening of 3' UTRs by alternative cleavage and polyadenylation activates oncogenes in cancer cells. *Cell*. 2009; 138:673–684. [PubMed: 19703394]
23. Eekels JJ, Pasternak AO, Schut AM, Geerts D, Jeeninga RE, Berkhout B. A competitive cell growth assay for the detection of subtle effects of gene transduction on cell proliferation. *Gene Ther*. 2012; 19:1058–1064. [PubMed: 22113311]
24. Kim KH, Sederstrom JM. Assaying Cell Cycle Status Using Flow Cytometry. *Curr Protoc Mol Biol*. 2015; 111:28.6.1–28.6.11. [PubMed: 26131851]
25. Ebert MS, Neilson JR, Sharp PA. MicroRNA sponges: competitive inhibitors of small RNAs in mammalian cells. *Nat Methods*. 2007; 4:721–726. [PubMed: 17694064]
26. Morabito F, Mosca L, Cutrona G, Agnelli L, Tuana G, Ferracin M, et al. Clinical monoclonal B lymphocytosis versus Rai 0 chronic lymphocytic leukemia: A comparison of cellular, cytogenetic, molecular, and clinical features. *Clin Cancer Res*. 2013; 19:5890–5900. [PubMed: 24036852]
27. Maura F, Cutrona G, Mosca L, Matis S, Lionetti M, Fabris S, et al. Association between gene and miRNA expression profiles and stereotyped subset #4 B-cell receptor in chronic lymphocytic leukemia. *Leuk Lymphoma*. 2015; 56:3150–3158. [PubMed: 25860243]
28. Mogilyansky E, Rigoutsos I. The miR-17/92 cluster: a comprehensive update on its genomics, genetics, functions and increasingly important and numerous roles in health and disease. *Cell Death Differ*. 2013; 20:1603–1614. [PubMed: 24212931]
29. Ren M, Cowell JK. Constitutive Notch pathway activation in murine ZMYM2-FGFR1-induced T-cell lymphomas associated with atypical myeloproliferative disease. *Blood*. 2011; 117:6837–6847. [PubMed: 21527531]
30. Turner N, Grose R. Fibroblast growth factor signalling: from development to cancer. *Nat Rev Cancer*. 2010; 10:116–129. [PubMed: 20094046]
31. Ornitz DM, Itoh N. The Fibroblast Growth Factor signaling pathway. *Wiley Interdiscip Rev Dev Biol*. 2015; 4:215–266. [PubMed: 25772309]
32. Zhou L, Liang X, Zhang L, Yang L, Nagao N, Wu H, et al. MiR-27a-3p functions as an oncogene in gastric cancer by targeting BTG2. *Oncotarget*. 2016; 7:51943–51954. [PubMed: 27409164]
33. Lai NS, Dong QS, Ding H, Miao ZL, Lin YC. MicroRNA-210 overexpression predicts poorer prognosis in glioma patients. *J Clin Neurosci*. 2014; 21:755–760. [PubMed: 24382515]
34. Pan Y, Meng M, Zhang G, Han H, Zhou Q. Oncogenic microRNAs in the genesis of leukemia and lymphoma. *Curr Pharm Des*. 2014; 20:5260–5267. [PubMed: 24479800]
35. Veronese A, Lupini L, Consiglio J, Visone R, Ferracin M, Fornari F, et al. Oncogenic role of miR-483-3p at the IGF2/483 locus. *Cancer Res*. 2010; 70:3140–3149. [PubMed: 20388800]
36. Petrocca F, Vecchione A, Croce CM. Emerging role of miR-106b-25/miR-17-92 clusters in the control of transforming growth factor beta signaling. *Cancer Res*. 2008; 68:8191–8194. [PubMed: 18922889]
37. Inomata M, Tagawa H, Guo YM, Kameoka Y, Takahashi N, Sawada K. MicroRNA-17-92 down-regulates expression of distinct targets in different B-cell lymphoma subtypes. *Blood*. 2009; 113:396–402. [PubMed: 18941111]
38. Mu P, Han YC, Betel D, Yao E, Squatrito M, Ogrodowski P, et al. Genetic dissection of the miR-17~92 cluster of microRNAs in Myc-induced B-cell lymphomas. *Genes Dev*. 2009; 23:2806–2811. [PubMed: 20008931]

39. Olive V, Bennett MJ, Walker JC, Ma C, Jiang I, Cordon-Cardo C, et al. miR-19 is a key oncogenic component of mir-17-92. *Gene Dev.* 2009; 23:2839–2849. [PubMed: 20008935]
40. Hong L, Lai M, Chen M, Xie C, Liao R, Kang YJ, et al. The miR-17-92 cluster of microRNAs confers tumorigenicity by inhibiting oncogene-induced senescence. *Cancer Res.* 2010; 70:8547–8557. [PubMed: 20851997]
41. Mi S, Li Z, Chen P, He C, Cao D, Elkahlon A, et al. Aberrant overexpression and function of the miR-17-92 cluster in MLL-rearranged acute leukemia. *Proc Natl Acad Sci U S A.* 2010; 107:3710–3715. [PubMed: 20133587]
42. Gao J, Li L, Wu M, Liu M, Xie X, Guo J, et al. MiR-26a inhibits proliferation and migration of breast cancer through repression of MCL-1. *PLoS One.* 2013; 8:e65138. [PubMed: 23750239]
43. Jiang X, Huang H, Li ZJ, Li YY, Wang X, Gurbuxani S, et al. Blockade of miR-150 Maturation by MLL-Fusion/MYC/LIN-28 Is Required for MLL-Associated Leukemia. *Cancer Cell.* 2012; 22:524–535. [PubMed: 23079661]
44. Jiang X, Bugno J, Hu C, Yang Y, Herold T, Qi J, et al. Eradication of Acute Myeloid Leukemia with FLT3 Ligand-Targeted miR-150 Nanoparticles. *Cancer Res.* 2016; 76:4470–80. [PubMed: 27280396]
45. Yang Z, Tsuchiya H, Zhang Y, Hartnett ME, Wang L. MicroRNA-433 inhibits liver cancer cell migration by repressing the protein expression and function of cAMP response element-binding protein. *J Biol Chem.* 2013; 288:28893–28899. [PubMed: 23979134]
46. Xiao F, Zhang W, Chen L, Chen F, Xie H, Xing C, et al. MicroRNA-503 inhibits the G1/S transition by downregulating cyclin D3 and E2F3 in hepatocellular carcinoma. *J Transl Med.* 2013; 11:195. [PubMed: 23967867]
47. Ren M, Qin H, Ren R, Tidwell J, Cowell JK. Src activation plays an important key role in lymphomagenesis induced by FGFR1 fusion kinases. *Cancer Res.* 2011; 71:7312–7322. [PubMed: 21937681]
48. Xu S, Ou X, Huo J, Lim K, Huang Y, Chee S, et al. Mir-17-92 regulates bone marrow homing of plasma cells and production of immunoglobulin G2c. *Nat Commun.* 2015; 6:6764. [PubMed: 25881561]
49. Mihailovich M, Bremang M, Spadotto V, Musiani D, Vitale E, Varano G, et al. miR-17-92 fine-tunes MYC expression and function to ensure optimal B cell lymphoma growth. *Nat Commun.* 2015; 6:8725. [PubMed: 26555894]
50. Psathas JN, Doonan PJ, Raman P, Freedman BD, Minn AJ, Thomas-Tikhonenko A. The Myc-miR-17-92 axis amplifies B-cell receptor signaling via inhibition of ITIM proteins: a novel lymphomagenic feed-forward loop. *Blood.* 2013; 122:4220–4229. [PubMed: 24169826]

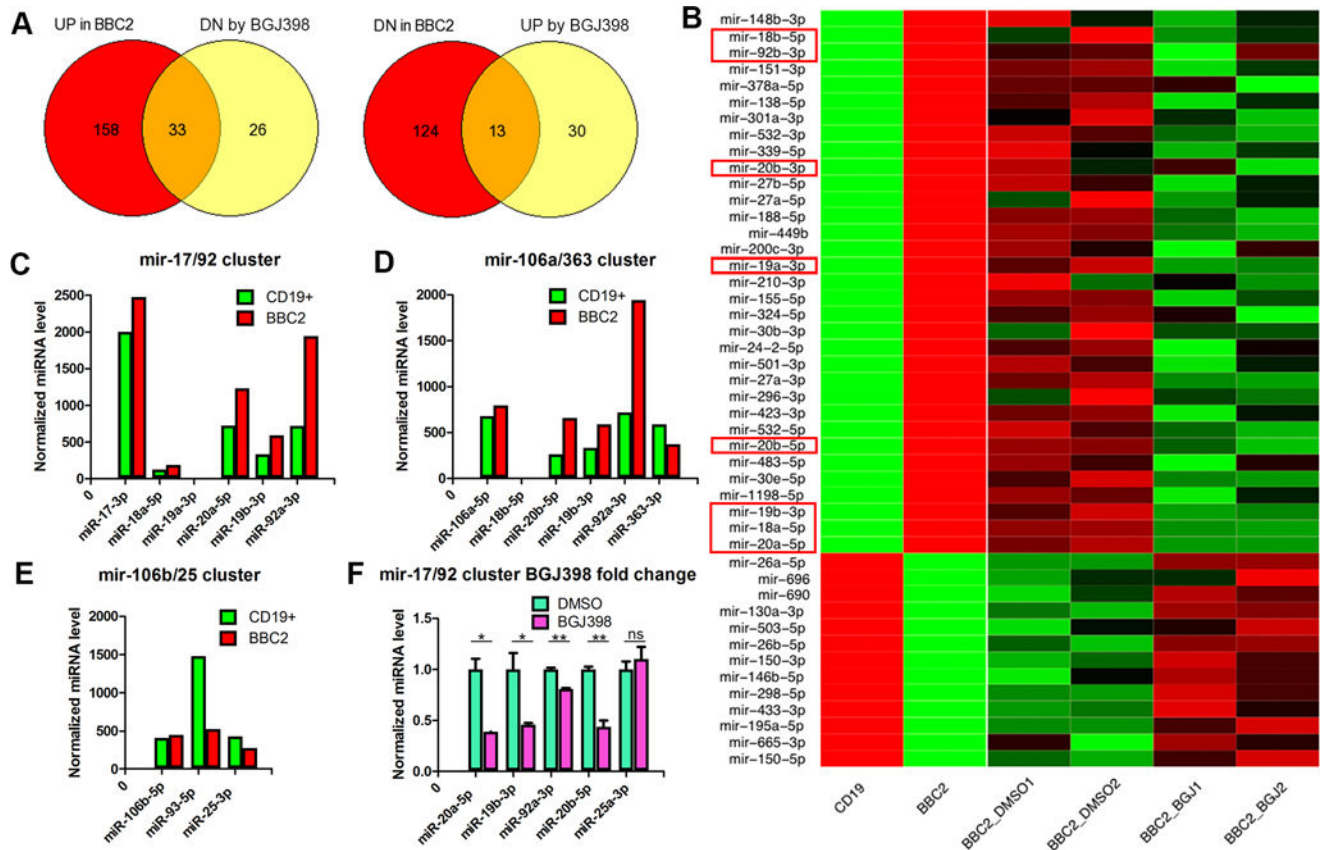


Figure 1. Identification of miRNAs regulated by chimeric FGFR1 kinase

MicroRNAs dysregulated in a comparison between normal CD19+ and BBC2 cells were identified and then VENN analysis (A) comparing upregulation or downregulation of these miRNAs following treatment of BBC2 cells with BGI398 identifies overlap for 46 core miRNAs. Hierarchical clustering (B) of these 46 core miRNAs, identifies miR-17/92 family members (highlighted in red boxes). Normalized expression levels for the six members of miR-17/92 in the comparison between CD19+ normal cells and BBC2 cells (C) as well as the paralogous human clusters miR-106a/363 (D) and miR-106b/25 (E) are shown. Changes in expression levels of the miR-17/92 cluster following BGI398 treatment of BBC2 cells are shown in (F). Statistical analysis was performed using the Student's t test. *p<0.05, **p<0.01, ns = not significant.

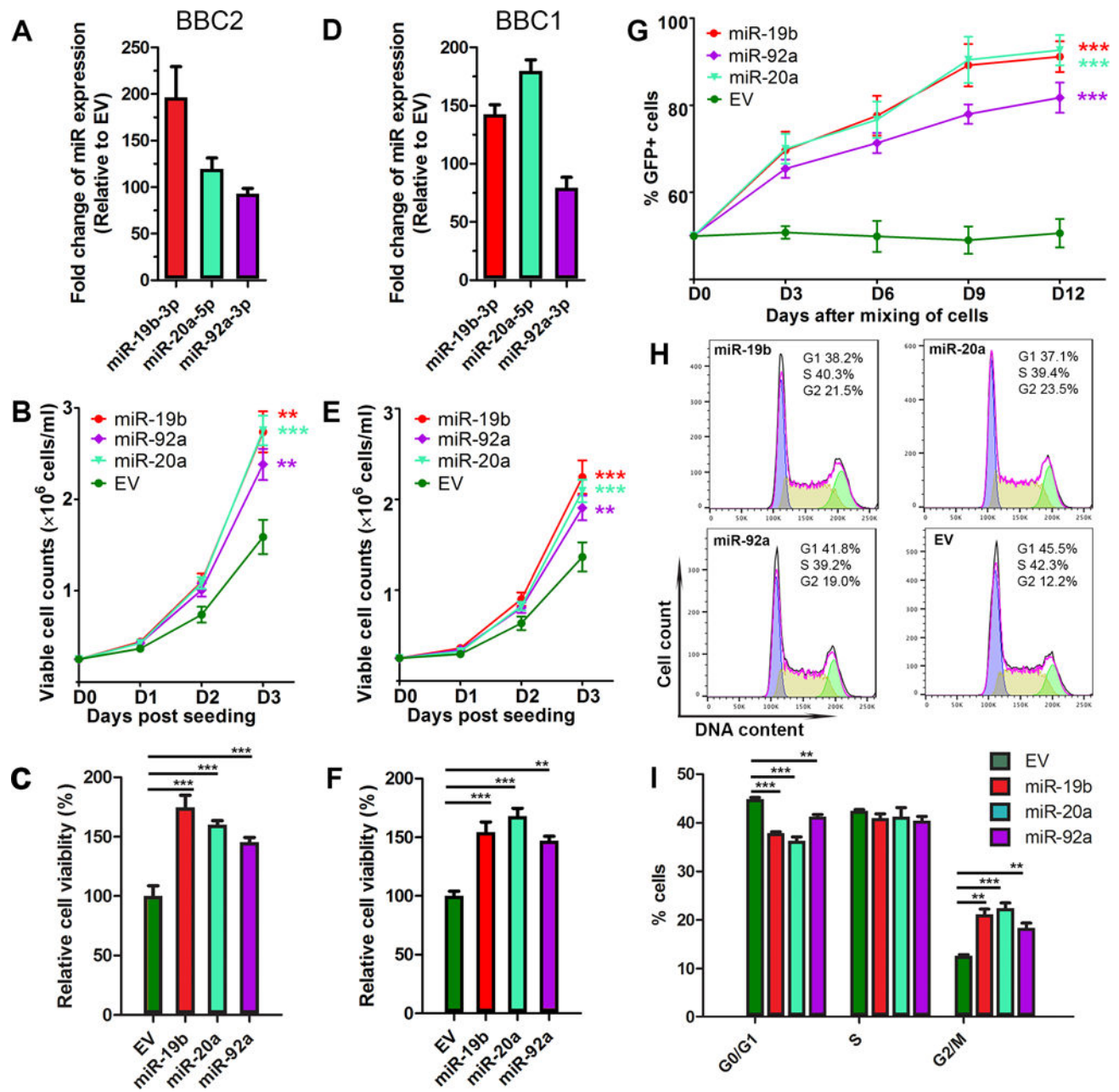


Figure 2. Forced expression of miRNA-17/92 promotes growth in BCR-FGFR1 expressing B-lymphoma cells

BBC2 cells expressing exogenous members of the miR-17/92 cluster show increased expression levels as determined using RT-PCR (A). Using trypan blue exclusion assays, all three members of the miR-17/92 cluster show a selective growth advantage in BBC2 cells by 72.4% ($p=1.20\text{e-}03$), 73.39% ($p=6.0\text{e-}04$) and 50.04% ($p=2.70\text{e-}03$) respectively (B) compared with cells expressing the empty vector (EV). This increased growth rate also correlated with CellTiter-Glo assays in BBC2 cells with increases of 74.76% ($p=1.93\text{e-}08$), 60.10% ($p=7.12\text{e-}11$) and 45.40% ($p=2.06\text{e-}11$) respectively, compared with empty vector controls (C). Similar cell growth (D) and viability (E-F) changes were seen in BBC1 cells

over-expressing BCR-FGFR1. In GFP competition assays (G), significant increases in GFP+ cells expressing the individual miRNAs (from ~50% to 91.19% ($p=1.27e-04$), 92.68% ($p=1.07e-04$) and 81.76% ($p=3.48e-04$) respectively) from miR-17/92 after 12 days. Representative flow cytometric plots (H) showing cell cycle distribution of BBC2 cells transduced with empty vector (EV) or miR-17/92 overexpressing retrovirus. Frequencies of cells at the different phases of cell cycle are shown (I), with significant increases in G2/M phase proportion in BBC2 cells expressing the individual miRNAs (from 12.63% to 21.17% ($p=1.40e-03$), 22.4 ($p=9.90e-04$) and 18.33% ($p=5.95e-03$) respectively). Means \pm SEMs of 3 independent experiments are shown by error bars throughout. T tests from experiments performed in triplicate. ** $p<0.01$, *** $p<0.001$.

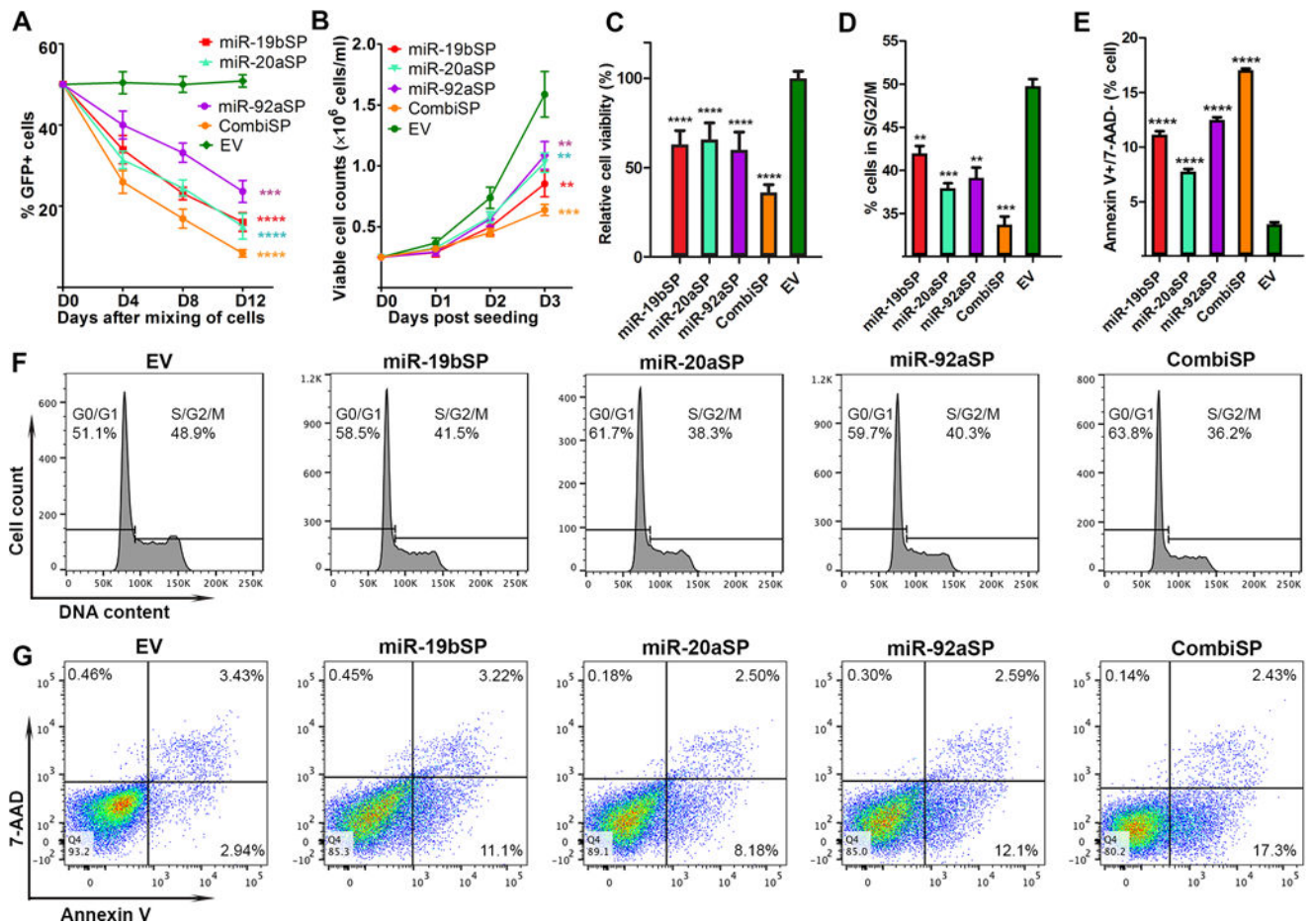


Figure 3. Inhibition of the miR-17/92 family members leads to suppression of cell growth and increases apoptosis

In GFP competition assays (A) suppression of the individual miR-17/92 family members in BBC2 cells, either individually or in combination, leads to significant suppression of cell growth. This change is mirrored by reduced cell viability assessed by both trypan exclusion assays at day 3 (B), with an average reduction of viability by 46.30% ($p=2.0\text{e-}03$), 35.34% ($p=4.40\text{e-}03$), 31.62% ($p=8.20\text{e-}03$) and 59.8% ($p=6.30\text{e-}04$), as well as CellTiter glow analysis (C), where the same transduced BBC2 cells showed decreased growth to 63.10% ($p=5.09\text{e-}10$), 65.94% ($p=1.35\text{e-}08$), 60.13% ($p=9.80\text{e-}10$) and 36.32% ($p=7.74\text{e-}12$) respectively, compared with empty vector transduced cells. Analysis of cell cycle in the miR-17/92 suppressed cells shows reduced proportions in the S/G2/M phases (D) with reductions from 49.77% to 41.97% ($p=2.80\text{e-}03$), 37.93% ($p=2.90\text{e-}04$), 39.13% ($p=1.90\text{e-}03$) and 33.73% ($p=2.0\text{e-}04$) respectively, and increases in apoptosis (E). Flow cytometric analysis of the cell cycle changes (F) and cell apoptosis (G) are shown. ** $p<0.01$, *** $p<0.001$, **** $p<0.0001$.

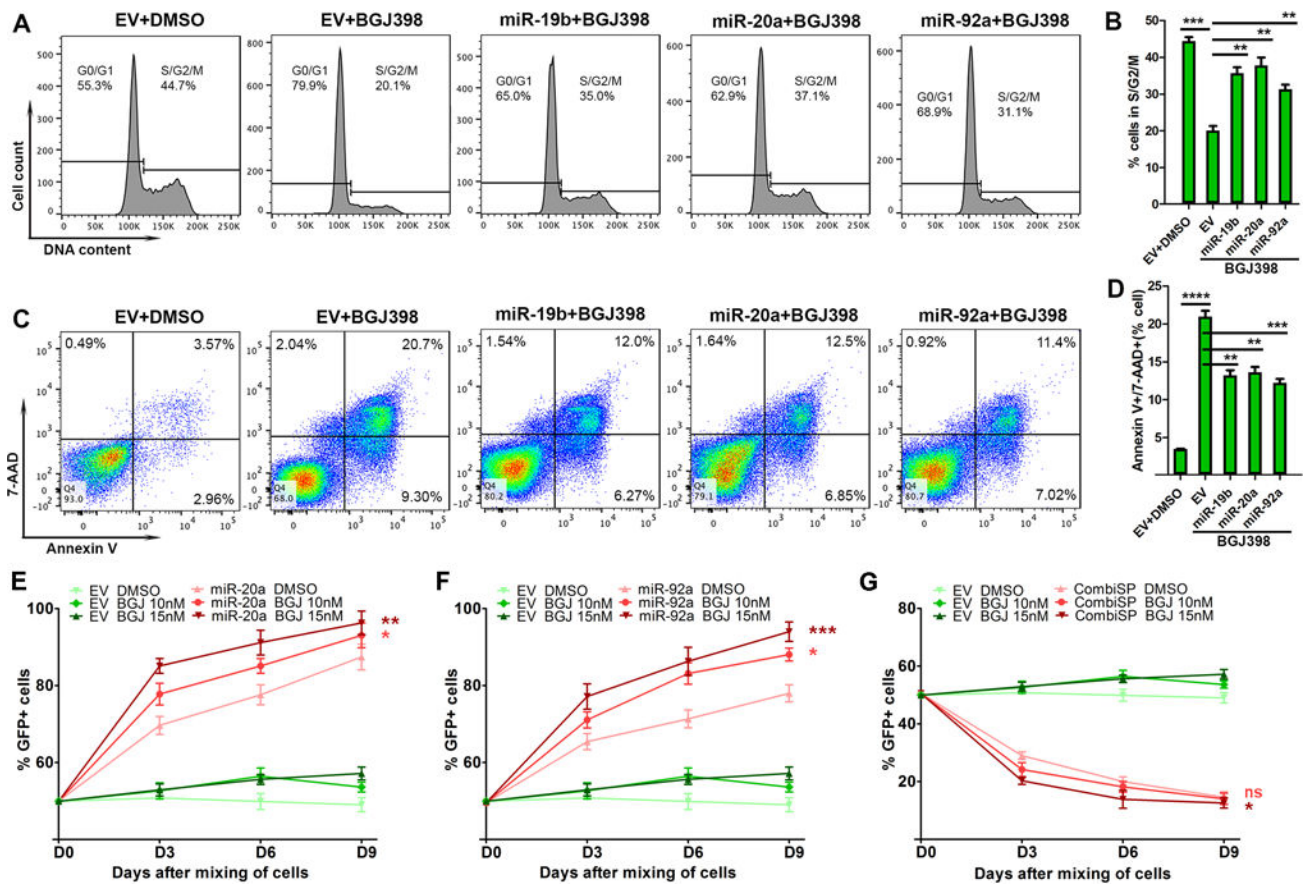


Figure 4. Forced expression of members of the miR-17/92 cluster can ameliorate BGJ398 suppression of FGFR1 activation

BBC2 cells treated with BGJ398 for 48 hours leads to reduction of cells in the S/G2/M phases of the cell cycle (A). Forced expression of the miR-17/92 family members in BBC2 cells ameliorates the effects of BGJ398 with increased numbers of cells in S/G2/M from 20.1% to 35.7% ($p=1.39e-03$), 37.8% ($p=1.97e-03$) and 31.3% ($p=3.10e-03$), respectively (B). Since BGJ398 leads to apoptosis, evaluation of annexin V and 7-AAD positive cells as a result of drug treatment (C) shows reduced Annexin V+/7-AAD+ cells from 20.97% to 13.2% ($p=1.70e-03$), 13.65% ($p=1.90e-03$) and 12.25% ($p=6.50e-04$), respectively, compared with parental cells expressing the empty vector (EV) (D). In GFP competition assay, overexpression of the miR-17/92 cluster provided a survival advantage in the presence of BGJ398 (E and F), while inhibition of its function using combined sponges sensitized the cells to BGJ398 treatment (G). ns, not significant, * $p<0.05$, ** $p<0.01$, *** $p<0.001$.

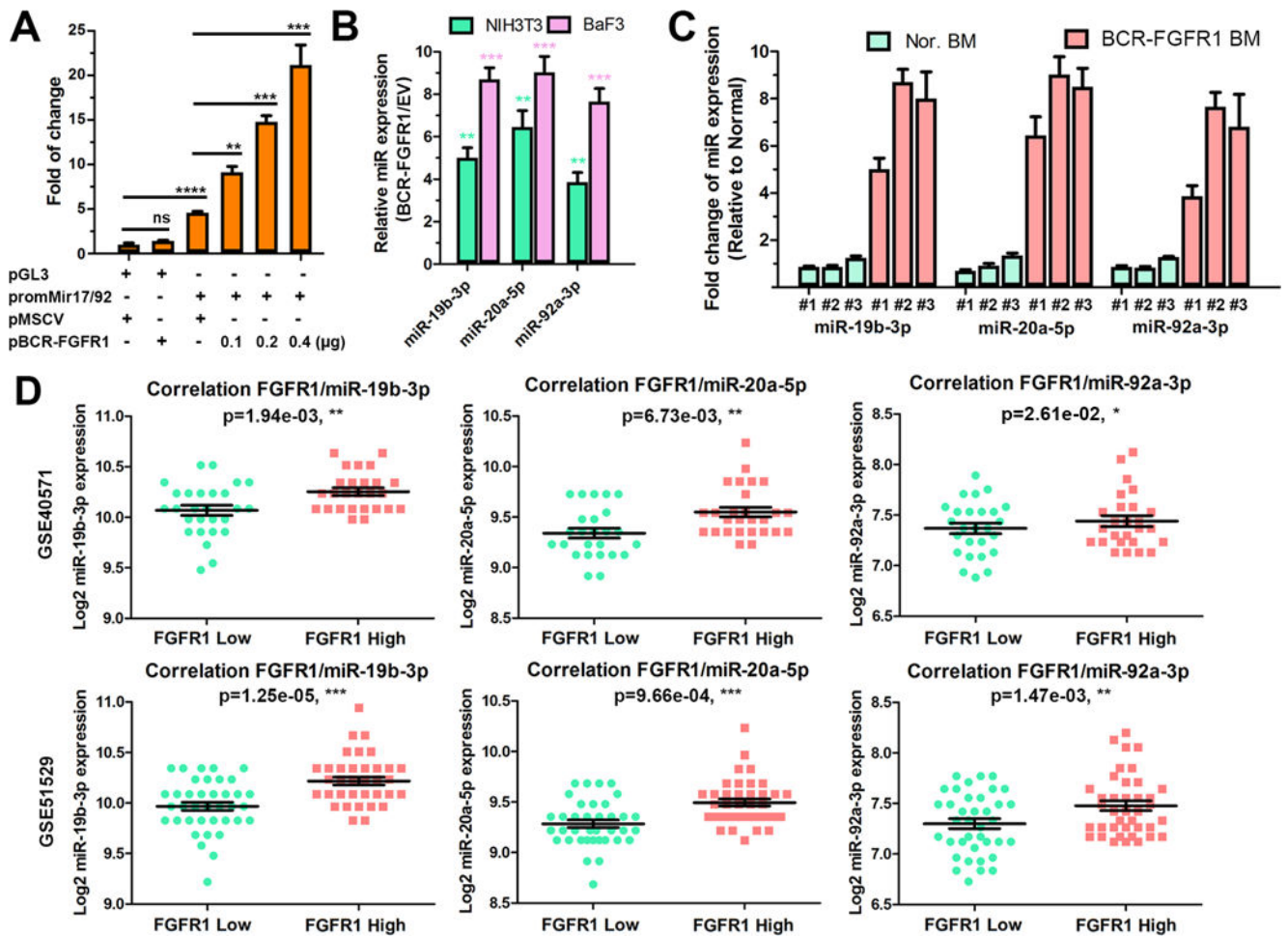


Figure 5. Regulation of miR-17/92 expression by FGFR1

(A) Luciferase promoter assays demonstrate a proportional increase of luciferase activity driven from the miR-17/92 promoter in the presence of increasing expression of BCR-FGFR1 compared with empty vector controls. Endogenous expression of miR-17/92 in either NIH3T3 or BaF3 cell stably expressing the BCR-FGFR1 shows increased expression compared with empty vector control (B). Comparison of miR-17/92 expression levels in B-lymphoma cells from the BCR-FGFR1 syngeneic mouse models shows significant increases compared with bone marrow from normal mice (C). Analysis of B-CLL tumors from two independent cohorts show significantly correlated expression levels of FGFR1 and miR-17/92 (D). Statistical analysis by Student's t test. ns, not significant, * $p < 0.05$, ** $p < 0.01$, *** $p < 0.001$, **** $p < 0.0001$.

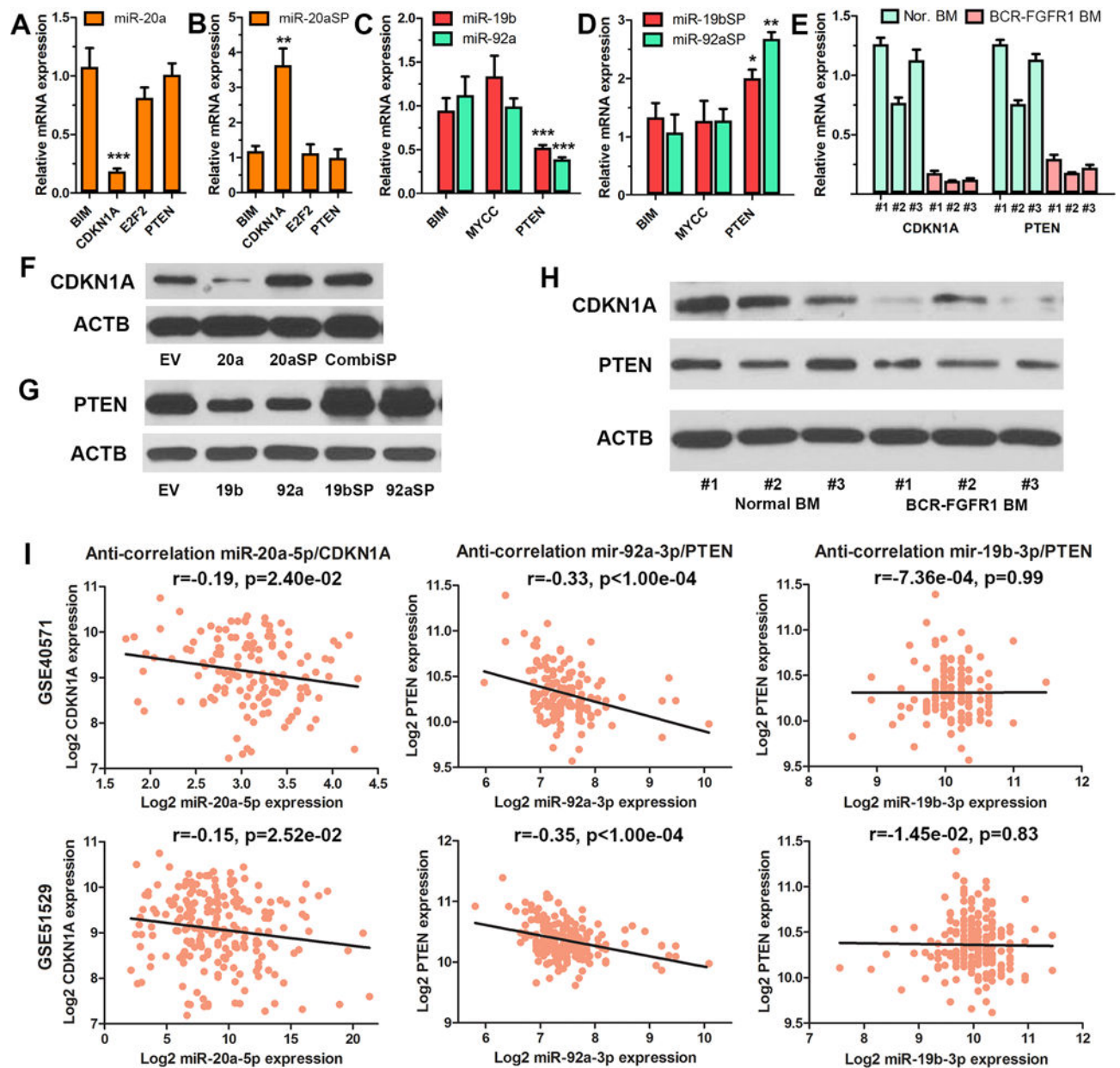


Figure 6. miR-17/92 targets CDKN1A and PTEN in FGFR1 driven leukemogenesis

Forced expression of miR-20a leads to reduced mRNA expression of CDKN1A (A), and inhibition of miR-20a by the corresponding sponge leads to increased expression (B) compared with empty vector controls. Overexpression of miR-19b and miR-92a leads to decreased PTEN mRNA expression (C) while inhibition of their expression leads to increased expression levels (D). Decreased expression levels of CDKN1A and PTEN are seen in BCR-FGFR1 primary lymphoma tissues from mouse models (E). Protein levels for CDKN1A and PTEN correlate with changes in mRNA expression levels in vitro (F, G) and in vivo (H), where expression in bone marrow cells from BCR-FGFR1 disease mice was reduced. All western blot experiments were repeated at least three times and the representative images were displayed. Anti-correlated expression of miR-20a-5p with

CDKN1A, and miR-92a-3p with PTEN, in two cohorts of CLL patients (I). * $p < 0.05$, ** $p < 0.01$, *** $p < 0.001$.

Author Manuscript

Author Manuscript

Author Manuscript

Author Manuscript

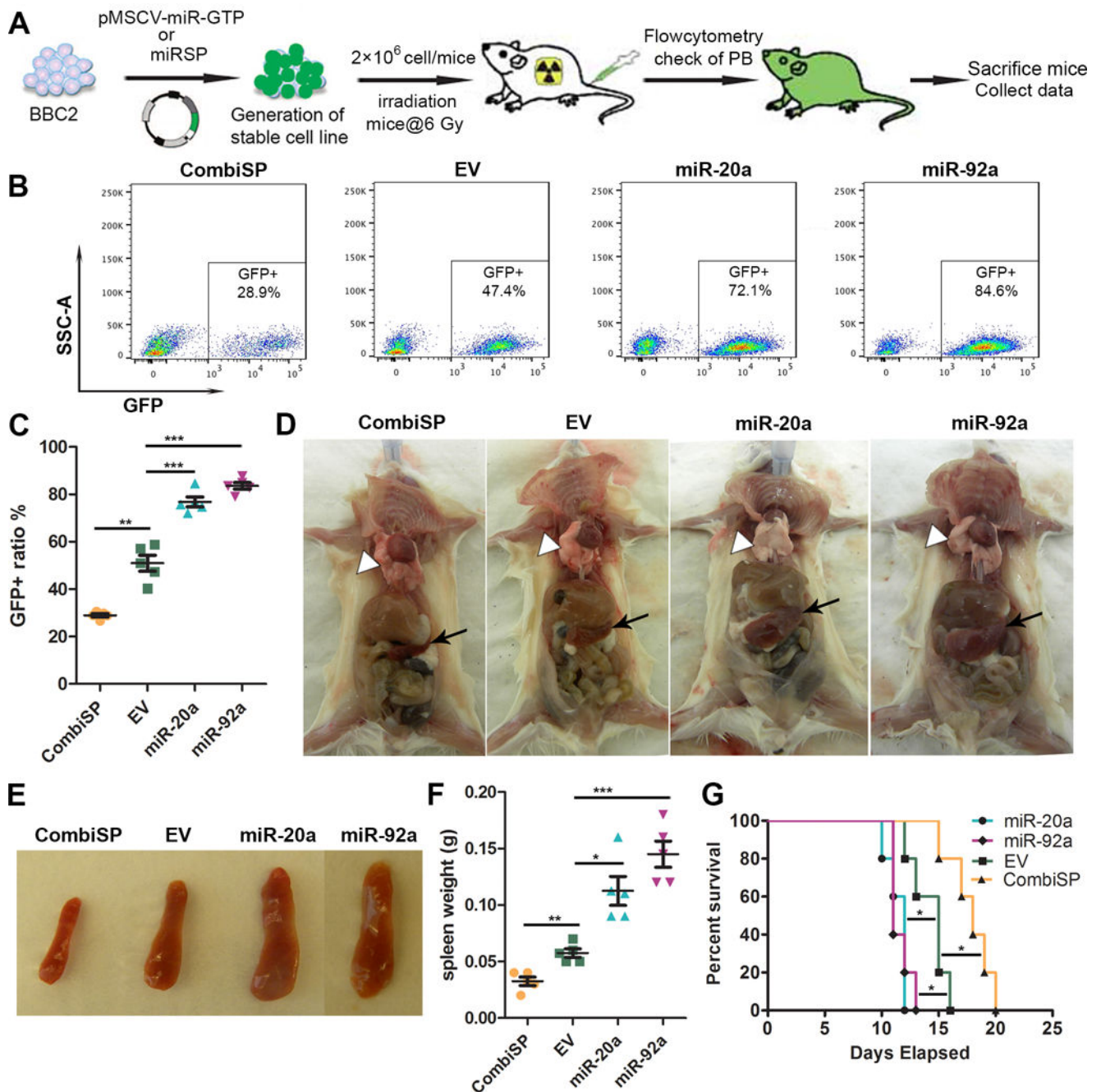


Figure 7. Manipulation of miR-17/92 affects FGFR1 driven leukemogenesis in vivo

(A) Schematic view of the procedures for syngeneic engraftment. Representative flow images show forced expression of miR-20a and miR-92a leads to increased proportions of GFP+ BBC2 cells in peripheral blood of engrafted mice after 1 week, and inhibition of the miR-17/92 cluster using the combined sponge (CombiSP) leads to a decrease in GFP+ BBC2 cells in peripheral blood (B), and the ratios of GFP+ cell as shown in (C). Autopsy of mice following injection of BBC2 cells expressing either the miR-17/92 combined sponge set or overexpressing miR-20a and miR-92a (D) shows reduced spleen size (arrows) in the sponge inhibited cells compared with empty vector control (EV), and increased lung

ischemia (arrowheads) and spleen size (arrows) in the BBC2 cells overexpressing the miRNAs. Overexpression of miR-20a and miR-92a leads to enlarged spleen size, while inhibition of expression (CombiSP) leads to decreased spleen size, compared with the empty vector control (E-F). Overexpression of miR-20a and miR-92a leads to accelerated disease progression, while inhibition of miR-17/92 function suppresses leukemogenesis development in vivo (G). * $p < 0.05$, ** $p < 0.01$, *** $p < 0.001$.

Author Manuscript

Author Manuscript

Author Manuscript

Author Manuscript